Vapor Thermodynamics and Fluid Merit for Pulsating Heat Pipe

Vadim S. Nikolayev✉– Iaroslav Nekrashevych
Université Paris-Saclay, CEA, CNRS, SPEC, 91191 Gif-sur-Yvette Cedex, France
✉ vadim.nikolayev@cea.fr

Abstract *In this communication, we discuss a theoretical description of the vapor phase thermodynamics in the pulsating heat pipe (PHP), to be used in numerical simulations. We advance a theory based on simulation results that allows us to derive a theoretical expression for a dimensionless quantity describing the vapor properties for a given fluid. One can use this quantity to evaluate the fluid merit for use in the PHP. This theory is confronted to the simulation results obtained with the PHP simulation code CASCO. We compare the merit of water, ethanol, and FC-72 and show that water possesses better properties for use in PHP.*

Keywords *pulsating heat pipe, oscillating flow, numerical simulation*

Highlights

- *Vapor thermodynamics at its fast state change is discussed.*
- *Model for vapor description is proposed for use in the pulsating heat pipe (PHP) simulation.*
- *Fluid merit number for PHP reflecting the vapor properties is proposed. It agrees with existing experiments.*
- *PHP simulations performed with code CASCO for different fluids agree with the merit number definition.*

1 INTRODUCTION

The pulsating (or oscillating) heat pipe (PHP) is a simple capillary tube bent into branches meandering between heat source and sink and partially filled with a two-phase, usually single component, working fluid. A pattern of multiple vapor bubbles separated by liquid plugs forms inside the tube. When the heat power is applied the whole train of bubbles and plugs begin to oscillate spontaneously due to evaporation and condensation occurring in the hot evaporator part and a cooler condenser, respectively. A combination of the latent heat transfer produced by the phase change and the convective boiling and condensation leads to a high performance of the PHP. Combined with its simplicity (thus high reliability and low cost) it makes PHP to be of high industrial potential. Last decades, researchers have extensively studied PHP [1] with dozens of research articles published each year in leading scientific journals. However the PHP functioning is intrinsically non-stationary, so very complex and is not completely understood. Simple PHP design tools are still absent and the only way to predict their functioning is the numerical simulation [2].

One of the most critical issue for the PHP modeling is the vapor phase thermodynamic state. In the most two-phase heat and mass exchange applications (like boiling [3]), the vapor is mostly at saturation so its compressibility can be neglected. The PHP case is different. Because its non-stationary functioning, the vapor state continuously varies, so both the current state and its change should be understood. The vapor at equilibrium with the liquid (at saturation) condenses at compression without giving an elastic response necessary for the oscillations.

The vapor state was studied experimentally by several research teams [4–7] by inserting the thermocouples into the PHP channel. Such studies are extremely delicate because of the difficulties to measure the vapor temperature during the oscillations. The convective heat exchange of the vapor with a thermocouple is weak and the measurement frequency is limited by the thermocouple thermal mass; the parasite radiative heat exchange with the internal surfaces of liquid and dry channel need to be carefully compared to the convective heat exchange. While such an evaluation has been done in some works [4, 7], it was neglected in the others thus reducing their data reliability. Gully et al. [4] have shown that the vapor is nearly always superheated in the evaporator and rarely approaches the coexistence curve; the vapor superheating ~ 10 K (with respect to $T_{sat}(p)$) was measured. Another team [5, 6] observed that, while the vapor is superheated in the evaporator part that remains dry during the oscillations, the measured T_v approaches T_{sat} in the areas where the liquid film covers the PHP channel walls in evaporator and adiabatic sections. However, the above thermocouple heat transfer analysis was not performed in these works. In addition, the cooling of the thermocouple by evaporation of liquid film left on it after the receding of liquid plug cannot be excluded. Recently, Mameli et al. [7] evaluated the vapor state in the condenser. Their data suggest that most of the time, $T_v < T_{sat}$ (i.e. metastable). It is difficult to understand from the physical viewpoint as the liquid films should always surround the vapor in evaporator and the metastability does not occur for condensation on the liquid surface. Mameli et al. expressed themselves reserves about these data accounting for the limitations on the measurement method. The question of the vapor thermodynamic state in the PHP thus remains open.

In the numerical modeling approaches, the state of a vapor bubble situating inside the PHP tube is usually described in terms of a single temperature T_v. Such a description is precise during the fast bubble motion, where the thickness of the thermal boundary layer developed inside the vapor is much smaller than the tube diameter due to the weakness of the vapor thermal conductivity [2]. In other cases, T_v corresponds to the spatially averaged vapor temperature.

Two PHP modeling approaches can be distinguished. In their pioneering article on the PHP modeling, Shafii et al. [8] assumed that the vapor behavior may be assimilated to that of the ideal gas that is described by the equation of state (EOS):

$$p = mR_vT_v/V. \quad (1)$$

DOI: 10.5545/sv-jme.2026.1779

Such an assumption was adopted in a large majority of modeling approaches.

Instead of using EOS, Eq. (1), Rouaze et al. [9] assumed the vapor to always remain at saturation evolving along the gas branch of coexistence curve (right part of the red curve in Fig. 1b), where

$$p = p_{sat}(T_v). \tag{2}$$

During the volume variation (vapor compression/dilatation) due to oscillations, vapor density ρ_{sat} changes. They find the new vapor temperature by inverting the $\rho_{sat}(T)$ curve (see Fig. 2 below). We note that the saturated vapor model can also create a kind of elastic response: when the vapor volume reduces at constant mass, ρ_{sat} increases (i.e. ρ_{sat}^{-1} decreases) and the pressure rises according to Fig. 1b together with the vapor temperature. Note that the such an assumption is hardly justified because it is not clear why the fluid cannot deviate from this particular trajectory (i.e., the coexistence curve) in the thermodynamic space. In addition, a change in vapor enthalpy appearing when the vapor evolves along the coexistence curve is not balanced; the energy conservation is not satisfied.

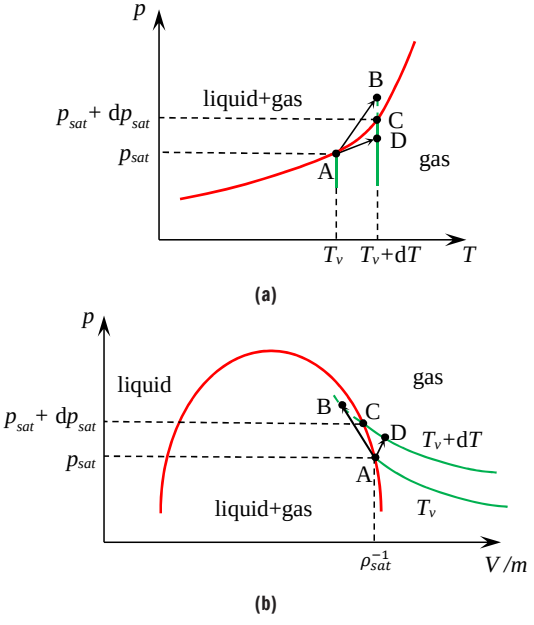

Fig. 1. Fluid phase diagram: a) in the $p-T$ coordinates, and b) in the $p-V$ coordinates; the isotherms in green and the coexistence in red

Many modeling approaches [10–15] try to reconcile these two models. On one hand, Eq. (1) describes the vapor state within them. On the other, they assume the channel wall-fluid heat exchange rate to be proportional to the difference $(T_w - T_v)$ of the wall and vapor temperatures. Note that in reality, the wall heat flux is spent mainly for the phase change, the rate of which is well known to be proportional to $(T_w - T_{sat})$ [3]. They justify the above assumption by the hypothesis that the vapor is saturated $(T_v = T_{sat})$.

The assumptions of superheated vapor and saturated vapor are however mutually exclusive if applied in dynamics. Indeed, the pressure of the saturated vapor is entirely defined by T_v (cf. Eq. (2)) rather than by T_v, m, and V (cf. Eq. (1)).

In this article we describe a modeling approach in which the vapor is allowed to change its state from superheated to saturated. This approach is used in the CASCO code (advanced PHP simulation code, the abbreviation of its name in French: Code Avancé de Simulation de Caloduc Oscillant) [16, 17]. In the second part of this communication we discuss the fluid merit number that appears to be linked to the vapor thermodynamic state evolution in PHPs.

2 VAPOR THERMODYNAMIC STATE

The phase diagram for common fluids at equilibrium is sketched in Fig. 1. The fluid equation of state (EOS, i.e. the set of thermodynamic states that can be occupied by the fluid) is a surface in the coordinates (p, V, T). The two phase (liquid-gas) coexistence region situates inside the red bell-shaped curve called coexistence curve as seen in the projection of this surface to the $p-V$ plane (Fig. 1b). Its projection to the $p-T$ plane is just a line called saturation curve shown in Fig. 1a. A part below the saturation curve corresponds to the gas phase (in which point D is situated), a part above, to the liquid. The point A (saturated vapor) situates at the coexistence curve. The gas state D is often referred to as superheated vapor because, at equal pressures, its temperature is higher than that of the saturated vapor, $T_D > T_{sat}(p_D)$, cf. Fig. 1a.

The above assumption about the vapor behavior similar to the ideal gas can be easily checked by comparing the density ρ_{sat} of saturated vapor calculated from Eqs. (1-2):

$$\rho_{sat} = \frac{p_{sat}(T_v)}{R_v T_v}, \tag{3}$$

to the experimental data (Fig. 2).

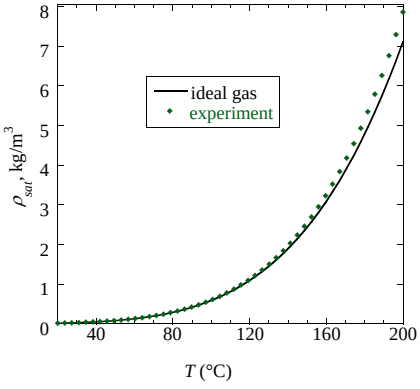

Fig. 2. Saturated vapor density (that corresponding to the boundary between the regions "gas" and "liquid+gas" in Fig. 1b) for water; the line corresponds to Eq. (3), while the characters are experimental data

One can see that the water vapor can be approximated with good accuracy by the ideal gas. For this reason, there is no need to use more sophisticated EOS forms.

When the superheated vapor is compressed or dilated (i.e. its volume changes), the vapor state follows EOS, Eq. (1), and the pressure responds, which creates a restoring force for the oscillation. However, to manage such events in the model, a solution proposed by Shafii et al. [8] can be used. The vapor state obeys Eq. (1) as long as $p < p_{sat}(T_v)$ (point D in Fig. 1). Once the pressure obtained with Eq. (1) becomes larger than $p_{sat}(T_v)$, the vapor pressure is imposed to be equal to p_{sat} and the vapor mass is made to be equal to $\rho_{sat}V$. The extra vapor mass condenses and is added to the liquid plug for mass conservation. In other words, the point B in Fig. 1 is shifted to the point C. This means that the subcooled vapor (which is a metastable or even thermodynamically unstable state) is not allowed in our model. This is justified from the physical point of view as discussed above.

The vapor temperature is not entirely homogeneous during vapor compression or expansion. Thermal boundary layers are developed near both the tube walls at temperature T_w and the liquid films at temperature T_{sat} covering the walls. The thickness of these layers is a complex yet unsolved issue. Direct numerical simulations [4] of the gas flow during oscillatory compression performed with ANSYS CFX software for oxygen at about 70 K showed a thickness of ~ 0.25 mm in the tube of 2 mm diameter. The vapor flow remains mostly laminar in the thermal boundary layers; turbulent mixing is absent near the wall. For this

reason, the vapor description with a unique temperature introduced above is reasonable. Because of a large temperature difference, the vapor heat exchange is mainly that with the dry wall area of the length L_d. The heat exchange coefficient is $U_v = Nu_v\lambda_v/d$ and the heat exchange rate is:

$$\dot{Q}_v = U_v \pi d L_d (T_w - T_v). \tag{4}$$

The above numerical calculation resulted in $Nu_v \simeq 6$. The heat exchange with the wetted wall area is usually smaller because of the smallness of the temperature difference $(T_{sat} - T_v)$; it is neglected here.

As mentioned above, while the superheated vapor behavior is entirely coherent with the experimental measurements and theoretical model presented by Gully et al. [4], the saturated state was observed by the Kim's group [5, 6].

3 VAPOR STATE CHANGE

The vapor energy equation is different for superheated vapor different thermodynamic state and should be derived from the first law of thermodynamics.

3.1 State Change in the Vapor Domain

When the vapor is superheated and obeys the ideal gas law, Eq. (1), Shafii et al. [8] showed that it can be described by the equation (see [18] for its detailed derivation):

$$mc_{vv}\dot{T}_v = R_v T_v \dot{m} - p\dot{V} + \dot{Q}_v \tag{5}$$

where dot means the time derivative. This equation can be reduced by using both EOS, Eq. (1) and Mayer's relation $c_{pv} = c_{vv} + R_v$ valid for the ideal gas:

$$\dot{p} = \frac{p}{T_v}\frac{\gamma}{\gamma - 1}\dot{T}_v - \frac{\dot{Q}_v}{V}, \tag{6}$$

where $\gamma = c_{pv}/c_{vv}$ is the adiabatic index.

If one neglects the heat transfer $\dot{Q}_v$ to the vapor, which is generally smaller than the effect of adiabatic compression, Eq. (6) can be integrated directly resulting in the adiabatic formula with no explicit dependence on time,

$$p = CT_v^{\frac{\gamma}{\gamma-1}}, \tag{7}$$

where the integration constant C is determined at the initial time moment. This approximation is convenient because reduces the number of differential equations and for this reason was used in many modeling approaches [19]. Such an approximation can be justified by the smallness of $\dot{Q}_v$ to the vapor (and can be indeed neglected) when calculating the overall heat transfer in the stable oscillation regime. However, in the vapor energy balance $\dot{Q}_v$ is important. In particular, $\dot{Q}_v$ term is essential for the start-up threshold determination [20, 21] so a more general form, Eq. (5), is kept in CASCO.

3.2 Saturated Vapor State Change

Besides the physical reasons discussed above, there is a practical reason requiring the introduction of the saturated vapor state. If one assumes that the vapor *always* satisfies the vapor domain EOS, Eq. (1), and *never* reaches the saturation state, the numerical simulation code can become unstable at large heat powers or large simulation times: T_v exhibits increasingly large temporal oscillation around more slowly changing T_w. A T_v rise causes a p rise through EOS, Eq. (1), which leads to T_{sat} increase. The vapor mass change rate is defined by the wall fluid heat flux so the vapor bubble mass change rate expression:

$$\dot{m} \sim (T_w - T_{sat}), \tag{8}$$

as explained above and can thus become negative. Because of Eq. (5) where $\dot{m}$ is the largest term, T_v decreases. However its decrease is much stronger than its previous increase. This effect can cause artificial oscillations that lead to huge vapor temperature (either positive or negative), and eventually the code crashes. To prevent it, the saturated vapor state needs to be introduced.

When the vapor is at saturation, it obeys the law as in Eq. (2). Most often, the saturation is attained in the condenser where there is no dry channel wall; the vapor sensible heat exchange $\dot{Q}_v$ with the environment is negligibly small so one can assume

$$\dot{T}_v = 0, \tag{9}$$

and the vapor pressure does not change either. All heat exchange leads to the phase change at the vapor-liquid interface, which maintains a constant vapor density $\rho_{sat}(T_v)$ and the vapor mass evolution obeys

$$\dot{m} = \dot{m}_{sat} \equiv \rho_{sat}\dot{V}, \tag{10}$$

instead of Eq. (8). In other words, the vapor condenses when compressed and vice-versa, evaporation occurs when the vapor is dilated. The condensed (or evaporated) liquid mass should be added to (or removed from) the liquid domain to conserve the total fluid mass.

The $\dot{m}$ definition in Eq. (10) cannot *always* be applied. Indeed, this would lead to impossibility for a bubble to leave the saturation state even during a strong film condensation (i.e. vapor mass reduction) or the bubble expansion. Within an adequate thermodynamic model, both these changes should lead to a pressure reduction so the vapor may possibly become superheated, cf. Fig. 1b). For this, an additional criterion based on the pressure change needs to be introduced; it is described hereafter.

Suppose the vapor is at saturation curve (point A in Fig. 1). While the vapor remains to be saturated, its evolution is governed by Eqs. (9,10), which means that the vapor state does not move from the point A. To determine if the vapor exits it, one needs to calculate the pressure change $\mathrm{d}p_{gas} = \dot{p}\mathrm{d}t$ under the hypothesis that the vapor is superheated, where $\mathrm{d}t$ is the time step and $\dot{p}$ is obtained from the EOS (with Eq. (6) for the ideal gas EOS). Since the point A situates at the coexistence curve, all the parameters in Eq. (6) have to be taken at the coexistence. In Fig. 1, the pressure change $\mathrm{d}p_{gas}$ corresponds to the transitions A→B or A→D. The corresponding T_v change is $\mathrm{d}T = \dot{T}_v\mathrm{d}t$ with $\dot{T}_v$ given by Eq. (5).

Two situations are possible. In the first case, the new vapor state would fall inside the coexistence curve (point B in Fig. 1). Evidently, in this case the vapor should remain to be saturated. In the second case (point D in Fig. 1), the vapor should quit the saturation state and become gas; the mass and temperature derivatives should now be defined with Eqs. (5, 8). Since the isotherm is a decreasing function (see Fig. 1), to distinguish two these cases, one needs to compare $\mathrm{d}p_{gas}$ with the change

$$\mathrm{d}p_{sat} = \left.\frac{\mathrm{d}p}{\mathrm{d}T}\right|_{sat}\mathrm{d}T, \tag{11}$$

that correspond to the transition A→ C in Fig. 1. The vapor stays at saturation while $\mathrm{d}p_{gas} \geq \mathrm{d}p_{sat}$. The vapor leaves the saturation state when $\mathrm{d}p_{gas} < \mathrm{d}p_{sat}$. Note that Fig. 1 apply to the case $\mathrm{d}T > 0$. One can easily check that the same criterion is valid for the case $\mathrm{d}T < 0$.

4 FLUID MERIT NUMBER

The above vapor state change criterion (i.e. a criterion of exiting the saturation state) reduces to

$$\frac{1}{N} - \frac{\dot{Q}_v}{\dot{T}_v V}\left.\frac{\mathrm{d}T}{\mathrm{d}p}\right|_{sat} < 1, \tag{12}$$

where

$$N = \frac{(\gamma - 1)T}{\gamma p_{sat}(T)}\left.\frac{\mathrm{d}p}{\mathrm{d}T}\right|_{sat}. \tag{13}$$

For a given fluid, the number N depends only on the temperature (Fig. 3) and exhibits a weak temperature variation. For some fluids

like FC-72, $N < 1$, while for others (ethanol or water), $N > 1$ over all the temperature range of interest.

The objective is to analyze the fluid merit for the PHP startup and stable functioning. This analysis is based on the PHP simulation results obtained with the numerical code CASCO [22] showing the importance of the bubble nucleation and growth in the evaporator section. In particular, the stable oscillations start when multiple vapor bubbles are generated in the evaporator. Consider a bubble freshly generated at a nucleation (hot) spot. A second bubble can be generated at the same hot spot while the first bubble is advected because of the liquid plug displacement during oscillating motion. Two bubbles become neighbors. The oscillations are amplified when both bubbles expand so a large pressure difference is created. However, when the growth of the second bubble leads to retraction and disappearance of the first, the oscillating motion is weak and the PHP performance is poor. However the growth of the second bubble leads inevitably to the compression of the first. At its birth, the vapor in the bubble is saturated. If the vapor remains saturated in the first bubble after generation of the second, the growth of the second bubble will lead to the contraction (because of condensation) of the first and its eventual disappearance. If, on the contrary, the vapor in the first bubble becomes superheated (i.e. elastic) it can resit to the compression and expand if evaporation into it occurs. For this reason, the ability of the vapor state change (saturated→superheated) is the major factor for the sustainment of oscillations.

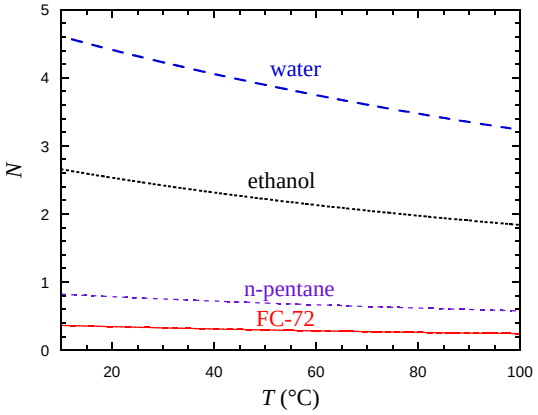

Fig. 3. Fluid merit number N related to the vapor compression

To analyze the vapor state change criterion in Eq. (12), the first (N^{-1}) term is more important than the second containing $\dot{Q}_v$. The mean value of the latter is generally small (because of the weak vapor heat exchange) and positive: the tube walls are hotter than vapor in the evaporator section. One can see that if $N < 1$, the bubbles can rarely exit the saturation state. The only effect that can drive them out of saturation is the vapor heat exchange. On the contrary, the bubbles of the fluids with $N > 1$ quit easier the saturation state helping to establish the stable oscillations. For this reason, N characterizes the fluid merit for usage in PHPs.

Such a fluid merit definition is coherent with the oscillation start-up threshold found analytically for the single-branch PHP [2, 21]. It was found that the oscillation start-up threshold decreases (which is beneficial) with $\mathrm{d}p/\mathrm{d}T|_{sat}$.

5 SIMULATION RESULTS

The simulation is performed with in-house CASCO software (French abbreviation for Code Avancé de Simulation du Caloduc Oscillant: advanced PHP simulation code [22,23] for three different fluids (water, ethanol and FC-72) for the flat PHP geometry shown in Fig. 4. where thin liquid films (in violet) cover the internal tube walls inside the vapor bubbles, except of the dry areas (in gray). The liquid plugs are shown in blue. The wall temperature is shown with the color varying from blue to red; its scale is indicated at the top. The round turns are not pictured for simplicity; black lines just connect equivalent points which correspond to the extreme points of each turn. An example of FC-72 in horizontal orientation for $P_e = 20$ W at $t = 140.198$ s is displayed.

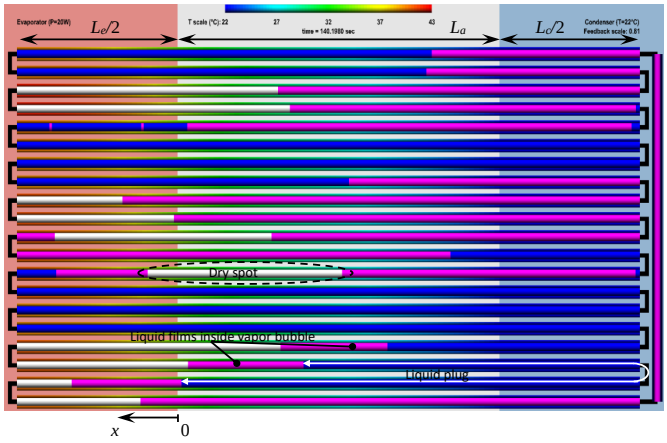

Fig. 4. The PHP geometry and the phase distribution pictured by the CASCO postprocessor.

The total power P_e injected into the evaporator and the temperature T_c at the internal tube walls are imposed in the simulation. Some portions of tube belong to the evaporator. The length of one portion is denoted L_e and their number is referred to as N_{turn}. To study the local fluid-tube thermal interaction, each of them is assumed to be heated independently and homogeneously, with the power P_e/N_{turn}. The PHP parameters are shown in Table 1.

Table 1. Parameters used for the simulation

Length of evaporator	$L_e = 126$ mm
Length of adiabatic section	$L_a = 126$ mm
Length of condenser	$L_c = 110$ mm
Number of turns	$N_{turn} = 10$
Feedback section length	$L_{fb} = 130$ mm
Filling ratio	$\phi = 0.5$
Inner diameter	$d = 1.4$ mm
Outer diameter	3.2 mm
Condenser temperature	$T_c = 22$°C
Tube material	Copper
Time step	10 µs
Tube mesh size	2 mm
Bubble deletion threshold	$L_{thr} = 10$ µm
Nucleated bubble length	$L_{nucl} = 500$ µm
Nucleation barrier	$\Delta T_{nucl} = 15$°C

The liquid film thickness δ is a fixed parameter in CASCO. It is calculated a posteriori from the average menisci velocity observed in simulations by using the Aussillous & Quéré formula [20, 24]. The thickness is not very sensitive to the velocity and can be fixed for each fluid. In present simulations, it is 40 µm for water, 80 µm for ethanol and 60 µm for FC-72. The performance of water and ethanol can be illustrated by Fig. 5.

One can see that in this particular situation both water and ethanol PHP show stable chaotic oscillations after an initial start-up period. In agreement with the above theory, the start-up of ethanol PHP in horizontal orientation is more difficult than of water PHP. In

particular, an initial evaporator overheating above the stable functioning temperature is needed to start-up the oscillations. In the beginning of evolution, most bubbles that existed initially disappear (the liquid plugs coalesce) when their length becomes smaller than L_{thr}. The system starts up by generation of multiple bubbles [22].

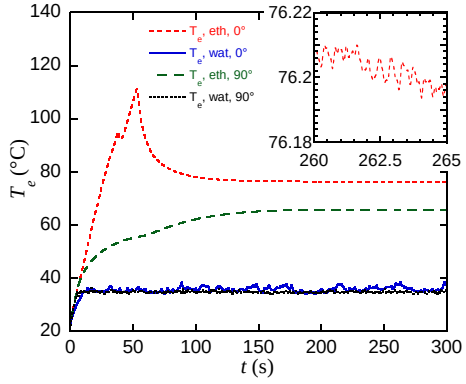

Fig. 5. Time evolution of the averaged over evaporator tube sections temperature T_e for water and ethanol in horizontal (0°) and vertical favorable (90°, evaporator under condenser) orientations for $P_e = 100$ W

Another manifestation of the difference between these fluids concerns different orientations. One can see that for water the performances in horizontal and vertical orientations are similar. It means that the pressure difference in the neighboring bubbles created during oscillation is much larger than the hydrostatic pressure (which is beneficial). This is not the case for ethanol, where the difference between horizontal and vertical orientations is striking.

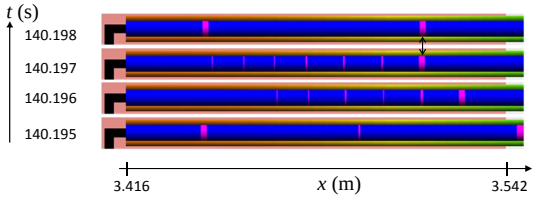

Fig. 6. Bubble generation and disappearance in the evaporator for the FC-72 case, the same as in Fig. 4, with the same T_w scale

The case of FC-72 is very different: for the horizontal orientation, stable oscillations appear only for a few particular choices of parameters. Usually the system dries out without attaining a stable oscillation regime. The initial stage dynamics is different from water or ethanol cases. After disappearance of the initial small bubbles and heating of the tube walls in evaporator section, bubble generation starts in long liquid plugs. At each time step, several bubbles of the size L_{nucl} are allowed to be nucleated sequentially once the difference between the wall temperature and the local saturation temperature exceeds the nucleation barrier (called also the superheating of the onset of nucleate boiling) [16]. As the vapor density is smaller, the ends of the original plug displace slightly during each nucleation event to accommodate the newly generated bubble volume. Therefore, each subsequent bubble nucleation leads to a compression of the previously nucleated bubbles. Because of a small $N < 1$ for FC-72, in many cases, a new nucleation leads to recondensation of the bubbles that were nucleated at the previous time step (Fig. 6). Instead of expanding (as the newly generated bubbles do in the water case [22]), they recondense. This process does not create oscillations so the PHP eventually dries out. In Fig. 6 four consecutive simulated time steps are shown. The evaporator part of the 16th from the bottom branch is presented. Most newly nucleated bubbles disappear at the next time step. The only bubble that survives two time steps is indicated with an arrow.

The fluid hierarchy provided by the number N (Fig. 3) agrees with the experimental study of Thapa et al. [25] who used several fluids in the same PHP prototype. Its geometry was close to ours. They showed that the water exhibited the best performance (*i.e.*, the smallest PHP thermal resistance). Ethanol was slightly worse, while FC-72 was the worst.

The number N characterizes a capacity of a given fluid to provide the oscillatory behavior. However, it is evident that the fluid merit is not defined solely by N. The liquid phase properties are also important. A 'good' fluid should have a small viscosity (for small viscous losses). High values of both latent heat and heat capacity of liquid are required to provide an efficient heat exchange.

Several attempts were undertaken in the past to propose an empirically-based fluid merit number accounting for both liquid and vapor properties. Probably the most often cited is that of Kim & Kim [26]:

$$M_{Kim} = \frac{c_{pl} R_v T_{sat}}{\nu_l h_{lv}} \left.\frac{\mathrm{d}p}{\mathrm{d}T}\right|_{sat}. \tag{14}$$

Note that this quantity is dimensional and thus does not result from a physical analysis. According to the graph [26] based on Eq. (14), water shows the smallest (*i.e.*, the worst) M_{Kim}, while FC-72, the largest. Although such an evaluation agrees with the experimental data of Kim & Kim [26], it is contrary to those of Thapa et al. [25]. Note that the geometries of their prototypes were entirely different. Such a comparison shows a necessity to search a physically based merit number (possibly including the PHP geometrical parameters), which is a task for the future research.

6 CONCLUSIONS

In conclusion, we propose here a model of the vapor behavior in the fast transients that occur in the PHP and derive the fluid merit factor. One notes that this factor corresponds only to the vapor phase properties and not to the liquid properties responsible for many other phenomena impacting the fluid merit like liquid viscosity and wetting. Such a merit factor allows us to explain the numerical simulation results obtained for three different fluids with the code CASCO. We show that, in agreement with the merit factor expression, FC-72 is generally worse for PHP applications than ethanol or water, which is confirmed by experimental studies of other researchers.

Nomenclature

c_{px}	specific heat at constant pressure of the phase, $x = (l, v)$ $[\frac{\mathrm{J}}{\mathrm{kg\,K}}]$
c_{vx}	specific heat at constant volume of the phase, $x = (l, v)$ $[\frac{\mathrm{J}}{\mathrm{kg\,K}}]$
d	PHP channel inner diameter [m]
h_{lv}	latent heat $[\frac{\mathrm{J}}{\mathrm{kg}}]$
L	length [m]
m	mass of vapor [kg]
N	fluid merit number
N_{turn}	number of PHP turns
Nu	Nusselt number
p	pressure [Pa]
$P, \dot{Q}$	power [W]
R	specific gas constant $[\frac{\mathrm{J}}{\mathrm{kg\,K}}]$
S	cross-section area [m^2]
T	temperature [K]
t	time [s]
U	heat transfer coefficient $[\frac{\mathrm{W}}{\mathrm{m}^2\,\mathrm{K}}]$

V	vapor bubble volume [m^3]
γ	vapor adiabatic index
Δ	difference
δ	thickness [m]
λ	heat conductivity [$\frac{W}{mK}$]
ν	liquid kinematic viscosity [$\frac{m^2}{s}$]
ρ	density [$\frac{kg}{m^3}$]
ϕ	volume fraction of liquid in PHP
a	adiabatic
c	condenser
d	dry
e	evaporator
f	liquid film
fb	feedback section (vertical in Fig. 4)
l	liquid
$nucl$	nucleation
sat	at saturation
thr	threshold
v	vapor
w	internal tube wall

References

[1] Marengo, M., Nikolayev, V. Pulsating heat pipes: experimental analysis, design and applications. J.R. Thome (ed.), *Encyclopedia of Two-Phase Heat Transf. and Flow IV, Volume 1: Modeling of Two-Phase Flows and Heat Transf.* 1–62 World Scientific (2018) Singapore **DOI:10.1142/9789813234406_0001**.

[2] Nikolayev, V. Physical principles and state-of-the-art of modeling of the pulsating heat pipe: A review. *Appl Therm Eng* 195 117111 (2021) **DOI:10.1016/j.applthermaleng.2021.117111**.

[3] Wei, L., Bois, G., Pandey, V., Nikolayev, V.S. Effect of contact line evaporation during nucleate boiling studied by multiscale numerical simulation. *Appl Therm Eng* 275 126690 (2025) **DOI:10.1016/j.applthermaleng.2025.126690**.

[4] Gully, P., Bonnet, F., Nikolayev, V.S., Luchier, N., Tran, T.Q. Evaluation of the vapor thermodynamic state in PHP. *Heat Pipe Sci Technol* 5 369–376 (2014) **DOI:10.1615/HeatPipeScieTech.v5.i1-4.410**.

[5] Noh, H.Y., Kim, S.J. Thermal characterization and optimization of pulsating heat pipes operating in a circulation mode. *Int J Heat Mass Transf* 115 1234–1246 (2017) **DOI:10.1016/j.ijheatmasstransfer.2017.09.004**.

[6] Jun, S., Kim, S.J. Experimental investigation on the thermodynamic state of vapor plugs in pulsating heat pipes. *Int J Heat Mass Transf* 134 321–328 (2019) **DOI:10.1016/j.ijheatmasstransfer.2019.01.053**.

[7] Mameli, M., Abela, M., Mazzini, J., Della Vista, D., Filippeschi, S. Novel experimental technique for the local thermodynamic analysis in pulsating heat pipes. *Int Commun Heat Mass Transf* 169 109825 (2025) **DOI:10.1016/j.icheatmasstransfer.2025.109825**.

[8] Shafii, M.B., Faghri, A., Zhang, Y. Thermal modeling of unlooped and looped pulsating heat pipes. *J Heat Transf* 123 1159–1172 (2001) **DOI:10.1115/1.1409266**.

[9] Rouaze, G., Marcinichen, J.B., Cataldo, F., Aubin, P., Thome, J.R. Simulation and experimental validation of pulsating heat pipes. *Appl Therm Eng* 196 117271 (2021) **DOI:10.1016/j.applthermaleng.2021.117271**.

[10] Dobson, R.T. Theoretical and experimental modelling of an open oscillatory heat pipe including gravity. *Int J Therm Sci* 43 113–119 (2004) **DOI:10.1016/j.ijthermalsci.2003.05.003**.

[11] Holley, B., Faghri, A. Analysis of pulsating heat pipe with capillary wick and varying channel diameter. *Int J Heat Mass Transf* 48 2635–2651 (2005) **DOI:10.1016/j.ijheatmasstransfer.2005.01.013**.

[12] Shao, W., Zhang, Y. Effects of film evaporation and condensation on oscillatory flow and heat transfer in an oscillating heat pipe. *J Heat Transf* 133 042901 (2011) **DOI:10.1115/1.4002780**.

[13] Cheng, P., Ma, H. A mathematical model of an oscillating heat pipe. *Heat Transf Eng* 32 1037–1046 (2011) **DOI:10.1080/01457632.2011.556495**.

[14] Mameli, M., Marengo, M., Zinna, S. Numerical model of a multi-turn closed loop pulsating heat pipe: effects of the local pressure losses due to meanderings. *Int J Heat Mass Transf* 55 1036–1047 (2012) **DOI:10.1016/j.ijheatmasstransfer.2011.10.006**.

[15] Ma, H. *Oscillating Heat Pipes*. Springer (2015) New York **DOI:10.1007/978-1-4939-2504-9**.

[16] Abela, M., Mameli, M., Nikolayev, V., Filippeschi, S. Experimental analysis and transient numerical simulation of a large diameter pulsating heat pipe in microgravity conditions. *Int J Heat Mass Transf* 187 122532 (2022) **DOI:10.1016/j.ijheatmasstransfer.2022.122532**.

[17] Abela, M., Mameli, M., Filippeschi, S., Nikolayev, V. Experimental and numerical studies of the pulsating heat pipe stopover regime. *Int J Heat Mass Transf* 247 127102 (2025) **DOI:10.1016/j.ijheatmasstransfer.2025.127102**.

[18] Nikolayev, V. Comment on "Flow and heat transfer of liquid plug and neighboring vapor slugs in a pulsating heat pipe" by Yuan, Qu, & Ma. *Int J Heat Mass Transf* 54 2226–2227 (2011) **DOI:10.1016/j.ijheatmasstransfer.2011.01.007**.

[19] Peng, H., Pai, P., Ma, H. Nonlinear thermomechanical finite-element modeling, analysis and characterization of multi-turn oscillating heat pipes. *Int J Heat Mass Transf* 69 424–437 (2014) **DOI:10.1016/j.ijheatmasstransfer.2013.10.041**.

[20] Nikolayev, V.S. Oscillatory instability of the gas-liquid meniscus in a capillary under the imposed temperature difference. *Int J Heat Mass Transf* 64 313–321 (2013) **DOI:10.1016/j.ijheatmasstransfer.2013.04.043**.

[21] Nikolayev, V.S. Effect of tube heat conduction on the single branch pulsating heat pipe start-up. *Int J Heat Mass Transf* 95 477–487 (2016) **DOI:10.1016/j.ijheatmasstransfer.2015.12.016**.

[22] Nekrashevych, I., Nikolayev, V.S. Effect of tube heat conduction on the pulsating heat pipe start-up. *Appl Therm Eng* 117 24–29 (2017) **DOI:10.1016/j.applthermaleng.2017.02.013**.

[23] Nikolayev, V.S. A dynamic film model of the pulsating heat pipe. *J Heat Transf* 133 081504 (2011) **DOI:10.1115/1.4003759**.

[24] Aussillous, P., Quéré, D. Quick deposition of a fluid on the wall of a tube. *Phys Fluids* 12 2367–2371 (2000) **DOI:10.1063/1.1289396**.

[25] Thapa, A., Chaudhary, M., Gallagher, R., Maroo, S.C. Thermal conductivity of water, ethanol, methanol and dielectric FC-72 in oscillating heat pipe. *Appl Therm Eng* 280 127966 (2025) **DOI:10.1016/j.applthermaleng.2025.127966**.

[26] Kim, J., Kim, S.J. Experimental investigation on working fluid selection in a micro pulsating heat pipe. *Energy Convers Manag* 205 112462 (2020) **DOI:10.1016/j.enconman.2019.112462**.

Acknowledgments *The financial contributions of ESA in the framework of the European Space Agency Microgravity Application Programme Project entitled Two-phase passive thermal devices for deployable Space Systems (TOPDESS, Project number 4000128640) and of CNES awarded through GdR MFA are acknowledged.*

Received *2026-04-24,* **revised** *2026-07-24,* **accepted** *2026-08-06* *as original scientific paper.*

Data availability *The data that support the findings of this study are available from the corresponding author upon reasonable request.*

Author contribution *Vadim S. Nikolayev: Funding Acquisition, Conceptualization, Methodology, Software, Investigation, Writing – Original Draft; Iaroslav Nekrashevych: Software, Data Curation, Writing – Original draft, Investigation.*

Termodinamika parne faze in primernost delovnega fluida za pulzirajočo toplotno cev

Povzetek *V tem prispevku obravnavamo teoretični opis termodinamike parne faze v pulzirajoči toplotni cevi (PHP), namenjen uporabi v numeričnih simulacijah. Na podlagi rezultatov simulacij razvijamo teorijo, ki omogoča izpeljavo teoretičnega izraza za brezdimenzijsko veličino, s katero je mogoče opisati lastnosti parne faze izbranega fluida. To veličino je mogoče uporabiti za oceno primernosti fluida za uporabo v PHP. Predlagana teorija je primerjana z rezultati simulacij, pridobljenimi s simulacijsko programsko opremo CASCO za PHP. Primerjana je primernost vode, etanola in fluida FC-72, rezultati pa kažejo, da ima voda ugodnejše lastnosti za uporabo v pulzirajočih toplotnih ceveh.*

Ključne besede *pulzirajoča toplotna cev, oscilirajoči tok, numerična simulacija*